Coherent Vortices in Strongly Coupled Liquids

Ashwin J.* and R. Ganesh†

Institute for Plasma Research, Bhat, Gandhinagar-382428, India

(Received 21 December 2010; published 30 March 2011)

Strongly coupled liquids are ubiquitous in both nature and laboratory plasma experiments. They are unique in the sense that their average potential energy per particle dominates over the average kinetic energy. Using ''first principles'' molecular dynamics (MD) simulations, we report for the first time the emergence of isolated coherent tripolar vortices from the evolution of axisymmetric flows in a prototype two-dimensional (2D) strongly coupled liquid, namely, the Yukawa liquid. Linear growth rates directly obtained from MD simulations are compared with a generalized hydrodynamic model. Our MD simulations reveal that the tripolar vortices persist over several turn over times and hence may be observed in strongly coupled liquids such as complex plasma, liquid metals and astrophysical systems such as white dwarfs and giant planetary interiors, thereby making the phenomenon universal.

DOI: 10.1103/PhysRevLett.106.135001 PACS numbers: 52.27.Gr, 05.10.−a, 52.27.Lw, 52.65.Yy

The emergence of coherent structures is a preeminent feature of both freely decaying and forced two-dimensional (2D) Navier-Stokes turbulence—a subject that has been of great interest to the physics community for the past three decades [1–3]. For decades, physicists have been fascinated by two main characteristics of these isolated coherent vortices: first, they are long-lived, which implies that they can last for several eddy turnover times and second, their ability to remarkably enhance transport length scales. A thorough understanding of the evolution and dynamics of these coherent structures is extremely important because of their relevance to large scale planetary fluid dynamics [4], astrophysical flows [5] and turbulent transport in fusion plasmas [6], to mention a few. In their seminal experimental work, Van Heijst and Kloosterziel showed the emergence of a coherent structure, the tripole, from an unstable cyclonic vortex in a homogeneously rotating fluid [7]. They found that the tripole was a very stable structure which could persist even in a highly sheared environment. Later Carton *et al.* [8] studied the generation of tripoles from the instability of axisymmetric monopoles through numerical simulations of barotropic equations. Since then, a great amount of work has been done to show the emergence of coherent vortices in the decay of an unstable axisymmetric vortex [9,10]. However, their emergence in such weakly coupled systems raise a few very important questions: Can coherent structures like tripoles emerge in strongly coupled liquids like complex plasmas, condensed matter systems and astrophysical systems such as white dwarfs, thereby making this phenomenon universal? Can we study the growth and saturation of these structures in laboratory experiments? What determines the lifetime of these vortices in such strongly coupled liquids? Recently, a study of Kelvin-Helmholtz (KH) instability in strongly coupled Yukawa liquids was reported using large scale molecular dynamics (MD) simulations [11], wherein, coherent vortices were seen to evolve in the nonlinear regime. An important question which immediately follows is the emergence and stability of isolated coherent vortices in strongly coupled liquids, which is the subject matter of the present work.

As we will be using a Yukawa liquid as a prototype model for a strongly coupled liquid, we take a closer look at the constituents of a typical Yukawa liquid or a complex plasma. A typical laboratory produced complex plasma is composed of weakly ionized gas and charged dust grains and can be modeled by a Yukawa potential $U = [Q^2/(4\pi\epsilon_0 r)]\exp(-r/\lambda_D)$, where Q is the dust charge, λ_D is the Debye length of the background plasma and r is the radial distance between two dust grains. In a strongly coupled complex plasma, the coupling parameter $\Gamma = Q^2/(4\pi\epsilon_0 a T_d)$ can be easily of the order 1 or larger (T_d and a are the dust temperature and the Wigner-Seitz radius, respectively). Complex plasmas offer a perfect testbed for numerous fluid dynamics studies and several authors have investigated the flows in complex plasma using both theoretical [12] and experimental methods [13]. It is important to note that the above said works rely on conventional fluid theories which have several limitations in presence of strong coupling effects, such as Bogoliubov-Born-Green-Kirkwood-Yvon (BBGKY) hierarchy closure issues [14]. To address these issues, several lower dimensional models have been proposed which attempt to approximately describe these strongly coupled systems [15]. As can be expected, the validity of these models across a wide range of coupling parameter remains unclear [16]. Hence in order to correctly describe these systems it becomes imperative to invoke ''first principles'' MD simulations which numerically solve the N body problem ''exactly.''

We have performed large scale MD simulations to study the emergence and evolution of coherent structures in a 2D strongly coupled Yukawa liquid. The Yukawa liquid can be fully characterized by two dimensionless numbers: (i) the

coupling parameter Γ, and (ii) the screening parameter $\kappa = a/\lambda_D$. The length, time and energy are normalized to a, $\Omega_{\rm pd}^{-1}$ and $Q^2/(4\pi\epsilon_0 a)$, respectively [11]. The plasma frequency is given by $\Omega_{\rm pd} = [Q^2 n/(2\epsilon_0 m a)]^{1/2}$, where n and m are the 2D dust number density and mass of the dust grain, respectively. We take a total of 2.304×10^5 grains for the 2D Yukawa liquid and periodic boundary conditions are employed along $\hat{x}$ and $\hat{y}$. The number density n of the Yukawa liquid is taken to be 1, which gives us a square region of size $L = 480$, centered at origin (0,0). The value of screening parameter κ in all our simulations is taken to be 0.5. The initial state is prepared by first connecting the 2D system to a Gaussian thermostat [17] and letting it evolve canonically for $200\Omega_{\rm pd}^{-1}$. We then remove the thermostat and let the system evolve for another $50\Omega_{\rm pd}^{-1}$ microcanonically. A standard leapfrog integrator with a time-step $\Delta T = 0.01\Omega_{\rm pd}^{-1}$ is employed such that the fluctuation in total energy is less than $10^{-4}\%$ over a typical run duration of $1000\Omega_{\rm pd}^{-1}$. The initial equilibrium is a thermally equilibrated Yukawa liquid at a desired Γ along with the following azimuthal velocity profile superposed on grain velocities (only once at time $t = 0$). Thus, we have, in polar coordinates (r, θ):

$$V_r = 0, \qquad V_\theta = V_0(1 + \Delta \cos(m_n\theta)) \tag{1}$$

where V_0 is the basic azimuthal velocity profile given by

$$V_0 = 2.25(r/l)\exp(-(r/l)^5) \tag{2}$$

m_n is the mode number excited, Δ is the perturbation amplitude taken as 0.1 and l is the scale length of vorticity variation which is taken to be 50. The corresponding basic vorticity profile is given as $\omega_0 = \nabla \times V_0 = -(4.5/l)[2.5(r/l)^5 - 1]\exp(-(r/l)^5)$. Clearly this basic vorticity profile exhibits two regions of oppositely signed vorticity from the center to the periphery. This profile has a zero net circulation ($\int_0^\infty \omega_0 r dr = 0$) and such vortices are also known as "shielded vortices." Our choice of velocity profile [Eq. (1)] is physically motivated by extensive laboratory experiments [7] and numerical simulations [8] in fluid dynamics. We define an eddy turnover time for the vortex as $T = 2\pi r_m/V_{0(r=r_m)}$, where r_m is the distance at which V_0 becomes maximum. Setting $(dV_0/dr)|_{r=r_m} = 0$, we get $r_m = (1/5)^{1/5} l$ and hence the turnover time $T \approx 170\Omega_{\rm pd}^{-1}$. At a time $t \approx 2.82$ T into the simulation, with initial $\Gamma = 50$ and $m_n = 2$ excited, a tripole vortex has emerged from the centrifugal instability (Fig. 1). It will be shown later (Fig. 4.) that $m_n = 2$ is the fastest growing mode, thus leading to the formation of a tripole. The snapshot shows the vorticity profile for the partial system ($\pm$ 175, $\pm$175) and one can clearly see the compact region having three aligned patches (a central core and the two accompanying satellites containing cyclonic and anticyclonic vorticity, respectively). The total circulation within the satellites is equal and opposite to the circulation within

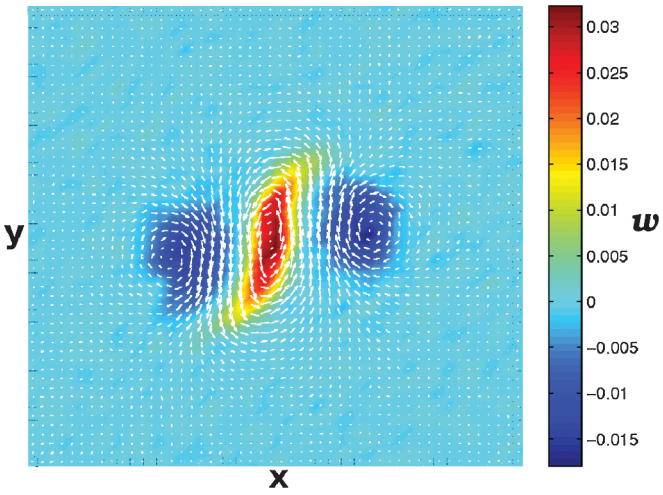

FIG. 1 (color). Tripole emerging at time $t = 2.82$ T, starting from an initial $\Gamma = 50$. The snapshot shows vorticity ($\boldsymbol{\omega} = \nabla \times \boldsymbol{v}$) plot for only a partial system ($\pm$ 175, $\pm$175). Grain velocities in the region are fluidized through a 45×45 grid to construct local vorticity. Blue and red regions correspond to negative and positive vorticity, respectively, and the color-map label shows the magnitude of local vorticity. Arrows indicating direction of local velocity are obtained by fluidizing the grain velocities over a 60×60 grid.

the central core. The tripole also exhibits a cyclonic rotation around the central core and is seen to be a very stable structure, sometimes persisting up to several turnover times. The magnitude of local vorticity ($\boldsymbol{\omega} = \nabla \times \boldsymbol{v}$) is indicated on a vertical color-map label. The local velocity $\boldsymbol{v}$ in the region is obtained by "fluidizing" the grain velocities over a 45×45 grid which amounts to averaging particle velocities locally to obtain fluid velocity at a grid point. At $\Gamma = 50$, the thermal velocity $v_{\rm th} = \sqrt{2/\Gamma} = 0.2$ and the ratio $v_{\rm th}/V_{0(r=r_m)} \approx 0.15$. It should be noted that the value of Γ close to the vortex boundaries decreases gradually in time due to shear induced heating [18] (not shown here). The superposed arrows indicating the local flow direction are obtained similarly from a 60×60 grid.

We have performed 2D MD simulations for the centrifugal instability of the profile given by Eq. (1) at three different values of initial coupling parameter Γ, namely $\Gamma = 1$, 50, 100. A given mode $m_n = 2$ is excited and coherent tripolar vortices are seen to emerge close to the end of the linear regime (Fig. 2). It is interesting to note the following facts: At strongest coupling ($\Gamma = 100$), the tripole vortex decays into two dipoles propagating in opposite directions, whereas, at $\Gamma = 50$, the tripole vortex is very stable and persists up to the entire duration of MD simulation (11.76 T). Such stable tripolar structures have been reported in early fluid simulations of barotropic equations [8,9]. Those fluids, however, were uncorrelated and without any strong coupling effects.

To understand the growth characteristic of a particular mode m_n, we study the time evolution of the perturbed

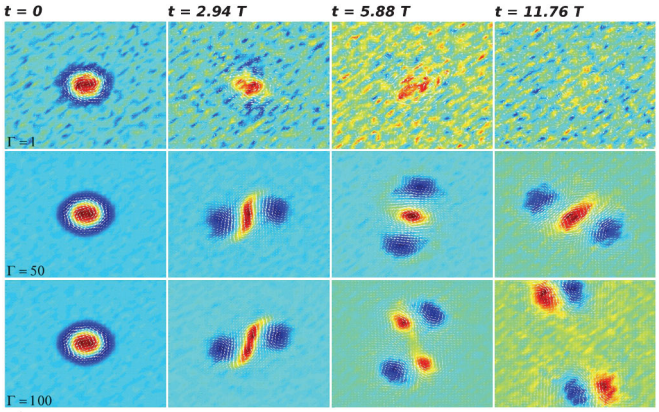

FIG. 2 (color). Time evolution of the vorticity profile for different values of initial Γ. The individual snapshots are shown for the full system (± 240, ±240) at times $t = 0$, 2.94, 5.88, and 11.76 T for three values of initial Γ, namely Γ = 1, 50 and 100 when a given mode ($m_n = 2$) is excited. Rows and columns show snapshots at constant Γ and t respectively. Blue and red regions correspond to negative and positive vorticity, respectively. At higher Γ's, the mode structures are more prominent and at the lowest Γ (highest temperature), the mode structures are weak and look diffused due to random thermal collisions between grains. It is interesting to note that for Γ = 50, a tripole persists (though rotating) throughout the total run duration, whereas, at Γ = 100, the tripole breaks into two propagating dipoles moving in opposite directions until $t = 11.76$ when the periodic boundaries come into play [see bottom-right].

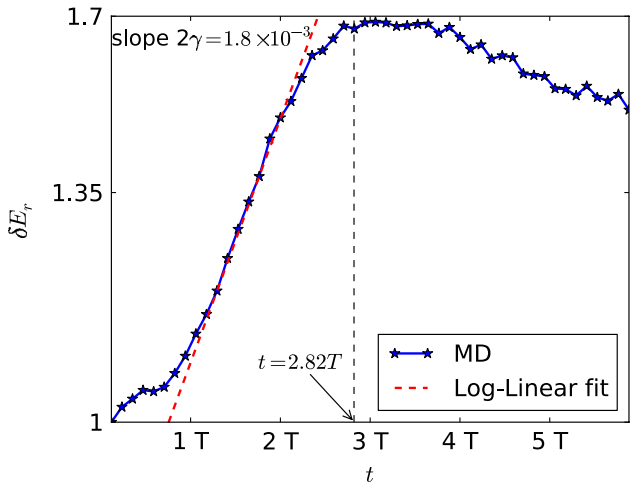

FIG. 3 (color online). Time evolution of perturbed kinetic energy along $\hat{r}$ [see text] on a log-linear scale for $m_n = 2$ and Γ = 50. The red dashed line shows a fit to the initial linear growth regime having slope 2γ. The vertical dashed line shows the onset of nonlinear saturation regime at $t = 2.82$ T which also coincides with the emergence of the fully developed tripole (Fig. 1).

kinetic energy along radial direction ($\hat{r}$) normalized to its initial value: $|\delta E_r| = [\iint (\hat{r} \cdot \boldsymbol{v}(t))^2 dxdy]/[\iint (\hat{r} \cdot \boldsymbol{v}(0))^2 dxdy]$. Starting from an initial state of $m_n = 2$ and Γ = 50, we plot this perturbed kinetic energy as a function of time and observe a linear growth eventually leading to a nonlinear saturation at late times (Fig. 3). The dashed line shows a fit to the initial linear growth regime. The slope (2γ) of this fit gives the growth rate of the centrifugal instability (γ). One clearly sees the onset of nonlinear saturation close to $t \approx 2.82$ T as shown by the vertical dashed line.

Although MD simulation results presented so far are an exact numerical solution to the N body problem and hence "first principles" in nature, it will be interesting to see if a lower dimensional fluid model can capture some of the underlying physics of the centrifugal instability. A well-known phenomenological fluid model for complex plasmas is the generalized hydrodynamic (GH) model [15,19,20] which attempts to describe strong coupling effects through the introduction of memory dependent viscoelastic coefficients. The GH model also has several limitations [21] and in the case of parallel shear flows, the comparison between MD simulations and GH model is at best only qualitative [18]. However, in light of the foregoing discussion, we obtain an analytical estimate of the linear growth rate of the centrifugal instability using the GH model. Thus, we write, the linear momentum equation for the incompressible dust fluid in the absence of dust-neutral collisions as [18]

$$(1 + \tau_m \partial_t)[(\partial_t + \mathbf{v}.\nabla)\mathbf{v} + (Ze/M)\nabla\phi + (1/\rho)\nabla P] = \nu\nabla^2\mathbf{v} + (1/\rho)(\zeta + \eta/3)\nabla(\nabla \cdot \mathbf{v}) \quad (3)$$

where ρ, $\boldsymbol{v}$, Ze and P are the mass density, fluid velocity, charge and pressure of the dust grains, respectively. η and ζ are the coefficients of shear and bulk viscosity, respectively. Kinematic viscosity is given by $\nu = \eta/\rho$ and ϕ is the electrostatic potential. The viscoelastic relaxation time τ_m is a measure of how memory effects due to strong coupling will influence the growth of instability in the medium. Taking curl of Eq. (3), we get the generalized hydrodynamic vorticity equation

$$(1 + \tau_m \partial_t)(\partial_t \boldsymbol{\omega} + (\boldsymbol{v} \cdot \nabla)\boldsymbol{\omega}) = \nu\nabla^2\boldsymbol{\omega}. \quad (4)$$

Equation (4) can be perturbed by writing velocity and the vorticity as

$$\boldsymbol{v} = (v_r', V_0 + v_\theta'), \qquad \boldsymbol{\omega} = \boldsymbol{\omega}_0 + \boldsymbol{\omega}', \quad (5)$$

where the quantities with primes are perturbed quantities. Using Eq. (5), the linearized z component of Eq. (4) becomes,

$$(1 + \tau_m \partial_t)[(\partial_t + (V_0/r)\partial_\theta)\omega' + v_r' D\omega_0] = \nu\nabla^2\omega' \quad (6)$$

Assuming continuity of mass ($\nabla \cdot \boldsymbol{v} = 0$), we introduce the stream-function $\boldsymbol{\Psi}' = (0, 0, \Psi')$ and write the perturbed velocities as $v_r' = (1/r)\partial_\theta\Psi'$ and $v_\theta' = -\partial_r\Psi'$. Using Eq. (6) and along with the fact that $\omega' = -\nabla^2\Psi'$, we get

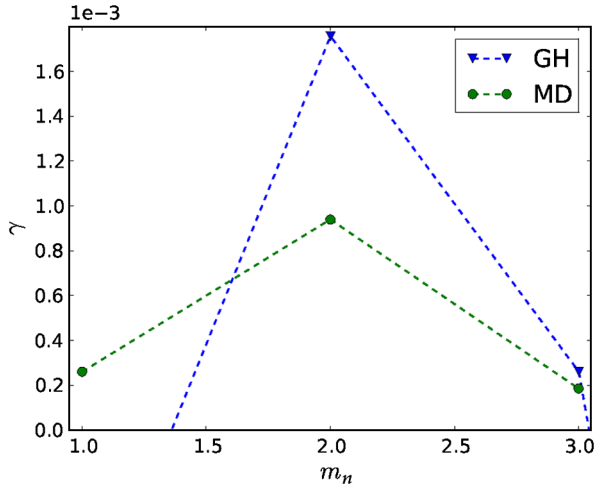

FIG. 4 (color online). Growth rate spectrum (solid circles) of centrifugal instability calculated from MD simulations at $\Gamma = 50$. Each point on the curve is obtained from the slope of the straight line fit to linear growth of the perturbed radial kinetic energy (Fig. 3). For comparison, the growth rates calculated from GH model [Eq. (8)] at $\nu(\Gamma) = 0.56$ and $\tau_m = 12$.

$$(1 + \tau_m \partial_t)[(\partial_t + (V_0/r)\partial_\theta)\nabla^2\Psi' - (1/r)(\partial_\theta\Psi')D\omega_0] = \nu\nabla^4\Psi'. \quad (7)$$

Taking normal mode ansatz: $\Psi' = \Phi' \exp(\gamma t + i m_n \theta)$, it is easily seen that Eq. (7) becomes

$$(1 + \tau_m\gamma)[(\gamma + i m_n V_0/r)(D_* D - (m_n/r)^2) - i(m_n/r)D\omega_0]\Phi' = \nu[D_* D - (m_n/r)^2]^2\Phi' \quad (8)$$

where $D = d/dr$ and $D_* = d/dr + 1/r$. Equation (8) is an eigenvalue equation and can be numerically solved for the eigenvalue γ. Typically, the viscoelastic relaxation time τ_m [19] depends on Γ and is given as $\tau_m = [4\eta/3 + \zeta]/[(3 - \Upsilon\mu_d)n + 4u/15]$ where, Υ is the adiabatic index, which for a 2D system is taken as 2 and μ_d is the compressibility. Thus, we find the value of $\tau_m \approx 12$ at $\Gamma = 50$ [18]. In Fig. 4, we show a comparison between the linear growth rate spectrum of the centrifugal instability directly obtained from MD simulations at $\Gamma = 50$ (solid circles) and the spectrum obtained from GH model [Eq. (8) and solid triangles]. We find that for the profile given by Eq. (2), the GH model (solid triangles) predicts only two unstable modes namely $m_n = 2, 3$. The GH growth rates though larger in magnitude appear to be in qualitative agreement with MD growth rates.

In conclusion, we have demonstrated for the first time, through large scale MD simulations, the emergence of isolated coherent tripolar vortices from the decay of unstable axisymmetric flows in strongly coupled Yukawa liquids. Linear growth rates of the instability are directly obtained from "first principles" MD simulations and emergence of coherent tripolar vortices in the nonlinear regime is reported. The tripoles formed are very robust and persist for several eddy turnover times. An attempt is made to compare the growth rates obtained from MD simulations with the GH fluid model. Several important questions can be addressed in the context of the present paper such as the enhancement of transport length scales due to these coherent tripolar vortices, inertial power laws and inverse cascade phenomena in 2D turbulent strongly coupled liquids. Our work expands the possibility of observing such tripolar vortices in laboratory experiments on complex plasmas, condensed matter systems and astrophysical systems, thereby vastly extending the generality of the phenomenon.

We thank Abhijit Sen for discussions.

*ashwin@ipr.res.in
†ganesh@ipr.res.in

[1] J. McWilliams, J. Fluid Mech. **146**, 21 (1984).
[2] B. Legras, P. Santangelo, and R. Benzi, Europhys. Lett. **5**, 37 (1988).
[3] N. Kukharkin, J. Sci. Comput. **10**, 409 (1995).
[4] J. Pedlosky, *Geophysical Fluid Dynamics* (Springer, New York, 1987).
[5] S. A. Balbus and J. F. Hawley, Rev. Mod. Phys. **70**, 1 (1998).
[6] Z. Lin, T. Hahm, W. Lee, W. Tang, and R. White, Science **281**, 1835 (1998).
[7] G. Van Heijst and R. Kloosterziel, Nature (London) **338**, 569 (1989).
[8] X. Carton, G. Flierl, and L. Polvani, Europhys. Lett. **9**, 339 (1989).
[9] P. Orlandi and G. van Heijst, Fluid Dyn. Res. **9**, 179 (1992).
[10] L. Barba and A. Leonard, Phys. Fluids **19**, 017101 (2007).
[11] J. Ashwin and R. Ganesh, Phys. Rev. Lett. **104**, 215003 (2010).
[12] N. D'Angelo and B. Song, Planet. Space Sci. **38**, 1577 (1990).
[13] Q. Z. Luo, N. D'Angelo, and R. L. Merlino, Phys. Plasmas **8**, 31 (2001).
[14] S. Ichimaru, *Basic Principles of Plasma Physics: a Statistical Approach.* (W. A. Benjamin, Inc., Reading, MA, 1964).
[15] S. Ichimaru, H. Iyetomi, and S. Tanaka, Phys. Rep. **149**, 91 (1987).
[16] *Strongly Coupled Coulomb Systems* edited by G J. Kalman, M. P. Rommel, and K. B. Blagoev (Plenum Press, New York, 1998).
[17] D. J. Evans, W. G. Hoover, B. H. Failor, B. Moran, and A. J. C. Ladd, Phys. Rev. A **28**, 1016 (1983).
[18] J. Ashwin and R. Ganesh, Phys. Plasmas **17**, 103706 (2010).
[19] M. A. Berkovsky, Phys. Lett. A **166**, 365 (1992).
[20] P. K. Kaw and A. Sen, Phys. Plasmas **5**, 3552 (1998).
[21] M. S. Murillo, Phys. Rev. Lett. **85**, 2514 (2000).